Title

The use of nanolipoprotein particles to enhance the immunostimulatory properties of innate immune agonists against lethal influenza challenge

Journal

Biomaterials, 34(38)

ISSN

0267-6605

Authors

Weilhammer, Dina R
Blanchette, Craig D
Fischer, Nicholas O
et al.

Publication Date

2013-12-01

DOI

10.1016/j.biomaterials.2013.09.038

Peer reviewed

Since January 2020 Elsevier has created a COVID-19 resource centre with free information in English and Mandarin on the novel coronavirus COVID-19. The COVID-19 resource centre is hosted on Elsevier Connect, the company's public news and information website.

Biomaterials 34 (2013) 10305–10318

Contents lists available at ScienceDirect

Biomaterials

journal homepage: www.elsevier.com/locate/biomaterials

The use of nanolipoprotein particles to enhance the immunostimulatory properties of innate immune agonists against lethal influenza challenge

Dina R. Weilhammer [a], Craig D. Blanchette [a], Nicholas O. Fischer [a], Shabnam Alam [b], Gabriela G. Loots [a, c], Michele Corzett [a], Cynthia Thomas [a], Cheri Lychak [a], Alexis D. Dunkle [a], Joyce J. Ruitenberg [d], Smita A. Ghanekar [d], Andrea J. Sant [b], Amy Rasley [a, *]

[a] Biosciences and Biotechnology Division, Lawrence Livermore National Laboratory, Livermore, CA 94551, USA
[b] David H. Smith Center for Vaccine Biology and Immunology, Department of Microbiology and Immunology, University of Rochester Medical Center, Rochester, NY 14642, USA
[c] School of Natural Sciences, University of California at Merced, Merced, CA 95340, USA
[d] BD Biosciences, 2350 Qume Drive, San Jose, CA 95131, USA

ARTICLE INFO

Article history:
Received 13 August 2013
Accepted 11 September 2013
Available online 27 September 2013

Keywords:
Immunomodulation
Nanoparticle
Drug delivery
Immunostimulation
Antimicrobial

ABSTRACT

Recent studies have demonstrated that therapies targeting the innate immune system have the potential to provide transient, non-specific protection from a variety of infectious organisms; however, the potential of enhancing the efficacy of such treatments using nano-scale delivery platforms requires more in depth evaluation. As such, we employed a nanolipoprotein (NLP) platform to enhance the efficacy of innate immune agonists. Here, we demonstrate that the synthetic Toll-like receptor (TLR) agonists monophosphoryl lipid A (MPLA) and CpG oligodeoxynucleotides (CpG) can be readily incorporated into NLPs. Conjugation of MPLA and CpG to NLPs (MPLA:NLP and CpG:NLP, respectively) significantly enhanced their immunostimulatory profiles both *in vitro* and *in vivo* compared to administration of agonists alone, as evidenced by significant increases in cytokine production, cell surface expression of activation markers, and upregulation of immunoregulatory genes. Importantly, enhancement of cytokine production by agonist conjugation to NLPs was also observed in primary human dendritic cells. Furthermore, BALB/c mice pretreated with CpG:NLP constructs survived a lethal influenza challenge whereas pretreatment with CpG alone had no effect on survival.

1. Background

Select classes of pathogenic organisms pose significant threats to public health due to the high levels of morbidity and mortality induced by very low infectious doses and their ease of transmissibility by aerosol [1]. For many of these organisms, efficacious therapies are not available or not optimal in the event of a bioterror attack or acute disease emergence. Vaccines, long considered the gold standard medical countermeasure for disease prevention, may not be available, or not suitable for widespread administration to the general public due to safety concerns [2]. Similarly, antimicrobial compounds may be insufficient to counter a wide range of unknown, deliberately altered, or drug-resistant pathogens and can potentially lead to resistance. As such, development of innovative approaches that allow for rapid responses to traditional and emerging pathogens is paramount. Recently, targeting the innate immune system to counter infection has been gaining attention as a therapeutic strategy [3–5]. The innate immune system has evolved over millennia to function immediately and non-specifically upon encountering pathogens [6], thus modulation of a single innate host resistance mechanism has the potential to offer broad-spectrum efficacy independent of pathogen identity. Furthermore, therapeutics targeting innate immunity would be less likely to promote the development of resistance, as the pathogen itself is not directly targeted.

Over the past fifteen years, pattern recognition receptors (PRRs), such as the Toll-like receptors (TLRs), have emerged as an intricate innate immune surveillance system that have evolved to detect a

* Corresponding author. Tel.: +1 925 423 1284; fax: +1 925 422 2282.
E-mail address: rasley2@llnl.gov (A. Rasley).

0142-9612/$ – see front matter © 2013 Elsevier Ltd. All rights reserved.
http://dx.doi.org/10.1016/j.biomaterials.2013.09.038

variety of invading pathogens expressing so-called pathogen-associated molecular patterns or PAMPs [6–8]. TLRs play a key role in the early steps of the immune response to infection, and robust TLR activation is critical for the downstream induction of a sustained adaptive immune response and pathogen clearance [9]. Importantly, the well-described association of TLRs with myriad infections underscores their importance as therapeutic targets and current research efforts are focused on clinically translating our understanding of TLRs and innate immunity [10–12]. Vaccine adjuvants are perhaps the most extensively explored application for TLR agonists, although there have been recent efforts exploring the use of TLR monotherapy to enhance host resistance to infection by a variety of pathogens [13–25]. However, there are significant limitations to the effectiveness of TLR agonists as stand-alone therapeutics, including marginal and short-lived protection, thus limiting their utility in both pre- and post-exposure scenarios. Furthermore, the dose required to afford protection in several of these studies was significantly higher than doses typically co-administered in combination with subunit antigens for vaccine applications [26], potentially raising toxicity concerns. Hence, strategies to improve the therapeutic index of TLR agonists *in vivo* are urgently needed.

Nanoparticles have been widely explored as delivery vehicles for immunotherapeutic applications [11,27], primarily to improve vaccine immunogenicity, reduce toxicities associated with high doses of adjuvants, improve pharmacokinetic profiles, and enhance stability of labile vaccine components. Although the functional indicator is ultimately heightened adaptive immune responses, nanoparticle-mediated enhancement of vaccine immunogenicity is likely due, at least in part, to heightened innate immune responses [28–31]. Indeed, several recent studies have demonstrated the prostimulatory effects of diverse nanoparticles on innate immune responses *in vitro* and *in vivo* [32–37]. In this study, we aimed to utilize nanolipoprotein particles (NLPs) to improve the efficacy of innate immune targeting therapeutics. NLPs are discoidal, nanometer-sized particles comprised of self-assembled phospholipid membranes and apolipoproteins [38,39]. Previously, we have described NLPs as a flexible vaccine platform for the co-localized administration of protein antigens and synthetic TLR agonists monophosphoryl lipid A (MPLA) and CpG oligodeoxynucleotides (CpG) [40]. Immunization with antigen:agonist:NLP complexes containing either influenza hemagglutinin or *Yersinia pestis* LcrV antigens and CpG or MPLA resulted in significantly higher antibody titers in mice against both antigens versus co-administration of antigens and agonists without NLP conjugation. Thus, NLPs have demonstrated effectiveness as a compatible platform for immune modulation strategies and have been used previously in other *in vivo* applications [41–44], supporting their broad utility.

Here, we investigated the interaction of NLP complexes with the innate immune system of mice and humans. Methods were developed for the incorporation and quantification of MPLA and CpG within NLPs. We then investigated the impact of NLP conjugation on innate immune responses to MPLA and CpG by measuring cytokine secretion, expression of immunoregulatory genes, and surface expression levels of key activation markers on antigen presenting cells (APCs). Stimulation of cytokine production was also investigated in primary human dendritic cells. Finally, we employed a mouse model of influenza in order to test the efficacy of CpG:NLP constructs at ameliorating infection.

2. Materials and methods

2.1. Reagents

Phospholipids 1,2-dioleoyl-*sn*-glycero-3-phosphocholine (DOPC), 1,2-dioleoyl-sn-glycero-3-[(N-(5-amino-1-carboxypentyl)iminodiacetic acid)succinyl] (nickel salt) (Ni-Lipid) and synthetic MPLA (PHAD™) were purchased from Avanti Polar Lipids, Inc. (Alabaster, AL). Cholesterol-modified CpG oligonucleotides were purchased as a custom order from Biosearch Technologies (Novato, CA). All mouse experiments were done utilizing the following sequence for Class B CpG: cholesterol-5′-TCCATGACGTTCCTGACGTT-3′ – all are phosphorothioate linkages. Experiments done in human cells utilized the following sequence for Class A CpG: cholesterol-5′ G*G*G*GACGACGTCGTGG*G*G*G*G-3′ – * denotes phosphorothioate linkages. It is worth noting that the cholesterol modified CpG compounds will be referred to as CpG below.

2.2. ApoE422k protein production

The expression clone to produce apoE422k, the N-terminal 22 kDa fragment of apolipoprotein E4 (apoE4), as a 6xHis and thioredoxin-tagged fusion construct was kindly provided by Dr. Karl Weisgraber. The apoE422k was expressed and purified using a similar protocol as previously described [38,39]. Endotoxin contamination was removed by reverse phase high-performance liquid chromatography (HPLC). ApoE422k was loaded onto a Vydac C4 column (22 × 250 mm, 10 μm; Grace Davidson, Deerfield, IL) and eluted with a 30–100% water/acetonitrile gradient (0.05% TFA, 7 ml/min). Fractions containing apoE422k were lyophilized, resuspended in pyrogen-free water, aliquoted, and stored at −20 °C.

2.3. Assembly of agonist-loaded nanolipoprotein particles (agonist:NLPs)

MPLA:NLPs and CpG:NLPs were assembled as described previously [40]. Briefly, for the MPLA:NLP assembly, the appropriate amount of chloroform-solubilized Ni-Lipid (35 mol%), DOPC (60–64.5 mol%) and MPLA (0.5–5 mol%) were determined prior to the experiment and added to a glass reaction vial. Chloroform was then removed using a stream of N_2 under agitation to form a thin lipid film. Lipids were solubilized in PBS buffer (137 mM NaCl, 2.7 mM KCl, 8 mM Na_2HPO_4 and 2 mM KH_2PO_4) using 40 mM sodium cholate. ApoE422k was added to the solubilized lipid suspension to a final lipid:apoE422k ratio of 80:1 (typically 150 μM apoE422k was used in the final assembly volume). For the CpG:NLP assembly, the lipid constituents were prepared as described above. CpG (hydrated from a lyophilized state using pyrogen-free water) was added to the solubilized lipid together with the apoE422K. Assemblies were dialyzed overnight against PBS to remove cholate and then filtered through a 0.22 μm spin filter to remove any large particulate matter. Samples were subsequently analyzed and purified by size exclusion chromatography (SEC) (Superdex 200 pg, HiLoad 16/600 column, GE Healthcare, Piscataway, NJ) in PBS buffer (1.0 ml/min flow rate). The apoE422k concentration in the NLP samples was determined using the Advanced Protein Assay Reagent (Cytoskeleton Inc., Denver, CO), using BSA as the standard. Free MPLA was prepared by first solubilizing MPLA in powder form in 100% DMSO at a concentration of 10 mg/ml. The solution was then diluted to 1 mg/ml in water and sonicated with a tip sonicator (Branson Sonifer, Model 250, Branson Ultrasonics, Danbury, CT) at the highest power until the suspension reached clarity. All buffers, eppendorf tubes and vials used during the assembly process were endotoxin-free. It is worth nothing that lipids containing a nickel chelating head group (Ni-Lipid) were included in all NLP assembly reactions, and while the NLPs generated for this study did not require the Ni functional group, we wanted to ensure that results obtained from this study would be applicable to ongoing NLP-based vaccine studies, in which a protein antigen is attached via the Ni-His tag interaction [40]. Additionally, a long-term objective of the approach described herein is to examine the effects of multiple immune modulators on a single NLP; thus, the Ni-Lipid was included in order to evaluate NLPs equipped for the attachment of His-tagged adjuvants, such as His-tagged flagellin [45].

2.4. Quantification of MPLA incorporation in NLPs

Incorporation of MPLA into NLPs was assessed by reverse phase HPLC by modifying published procedures [46]. Briefly, 20 μl concentrated NLP stocks containing MPLA were speed-vacuumed until dry. Lipophilic components were extracted from the dry pellet with extraction buffer (90% MeOH, 10% $CHCl_3$) for 2 h under constant agitation. After centrifugation to pellet insoluble material, the solvent was transferred to glass injection vials for HPLC analysis (Shimadzu Precision HPLC system). MPLA standards were prepared in extraction buffer (5–150 μg/ml). Samples and standards were analyzed on a Luna C18 column (4.6 × 150 mm, 5 μm; Phenomenex, Torrence, CA) using a constant flow rate (1 ml/min, 30 °C). Gradient conditions of Buffer A (95% methanol, 5% water, 0.1% TFA) and Buffer B (100% isopropanol, 0.1% TFA) were as follows: 0 min, 5% B; 10 min, 40% B; 18 min, 40% B; 20 min, 80% B; 28 min, 80% B; 35 min, 5% B. MPLA was detected using an evaporative light scattering detector (ELSD) (40 °C, gain 11). Sample concentrations were calculated using a quadratic curve fit of calibration standards ($r^2 = 0.998$) using Shimadzu LabSolutions (v5.51) software. In a typical assembly, mass ratios of E422k to MPLA were *ca.* 15:1.

2.5. Quantification of CpG incorporation in NLPs

Incorporation of CpG into the NLPs was quantified using Quant-iT OliGreen dye (Invitrogen, Carlsbad, CA), which is widely used to quantify ssDNA. Briefly, standard

CpG solutions (16, 8, 4, 2, 1 μg/ml) were prepared and diluted in TE buffer (10 mM Tris–HCl, 1 mM EDTA, pH 7.5). The CpG:NLP samples were also diluted in TE buffer. 100 μl of the sample and CpG standards were added to 96-well plates in duplicate, followed by the addition of 100 μl of the aqueous working solution of the Quant-iT OliGreen reagent. The fluorescence of the sample was then measured at an excitation and emission wavelength of 480 nm and 520 nm, respectively. Since the standards were not traditional ssDNA (CpG contains a phosphorothiolated back bone), the standard curve was sigmoidal rather than linear. Therefore, the standard curve was established by fitting the standards to a sigmoidal function, which was used to calculate the CpG concentration in the CpG:NLP. It is worth noting only fluorescence values that were within the sloping region of the sigmoidal function were used to calculate CpG concentrations since values in the saturation region were more prone to error. To ensure that the NLP itself did not affect the fluorescence emission of the Quant-iT OliGreen dye, the fluorescence values of free CpG standards and CpG standards in the presence of NLPs were compared, and no significant differences were observed. The number of CpG molecules per NLP was then calculated using the experimentally determined apoE422k protein concentration while assuming that each NLP contains 6 apoE422k proteins [39]. In a typical assembly, mass ratios of E422k to CpG were *ca.* 4:1.

2.6. Endotoxin quantification

Quantification of endotoxin levels was conducted using the Endosafe®-PTS™ (Charles River, Charleston, SC) endotoxin testing system based on Limulus Amebocyte Lysate (LAL) assay. All purified apoE422k contained less than 2 EU/mg of protein. Final NLP preparations contained between 20 and 100 EU/mg, based on apoE422k content.

2.7. Mice

All *in vivo* and *in vitro* experiments using *ex vivo* isolated mouse cells, other than influenza challenge experiments, were performed at Lawrence Livermore National Laboratory in PHS-assured facilities in accordance with guidelines set by the Animal Care and Use Committee. BALB/c male mice (4–8 weeks) were obtained from Harlan Laboratories (Livermore, CA). Influenza infection experiments were performed at the University of Rochester with female BALB/c (A^d, E^d) mice purchased from National Cancer Institute-Frederick (Frederick, MD). The mice were maintained in the specific pathogen-free facility at the University of Rochester, according to institutional guidelines, and infected at 8–16 weeks of age.

2.8. Cell culture

J774A.1 (J774) cells were maintained in Dulbecco's Modified Eagle's Media (DMEM; Invitrogen) supplemented with 10% heat inactivated fetal bovine serum (FBS; Invitrogen), 1% penicillin/streptomycin mix (Invitrogen) at 37 °C 5% CO2. Thioglycollate elicited primary peritoneal macrophages (pMP) were isolated as previously described [47]. Briefly, male BALB/c mice were injected intraperitoneally (IP) with 1 ml of 4% (w/v) Brewers Thioglycollate broth and five days post injection, mice were euthanized and peritoneal macrophages isolated by peritoneal lavage. Isolated macrophages were allowed to adhere to tissue culture plates in RPMI (Invitrogen) + 10% FBS + 1% penicillin/streptomycin mix overnight at 37 °C before non-adherent cells were washed off and adherent cells placed into experimental conditions. For all *in vitro* assays unless otherwise noted, cells were incubated with NLPs in Opti-MEM media (Invitrogen) with no added supplements.

2.9. In vitro analyses of NLP uptake

ApoE422k protein was labeled with Alexa Fluor 488 (AF488) dye (amine-reactive succinimidyl ester, Invitrogen) by incubating the assembled NLPs with AF488 at a NLP to dye molar ratio of 5 for at least 2 h. The reaction was performed in PBS buffer containing 5 mM sodium bicarbonate (pH 8.2). After completion of the reaction, 10 mM Tris (pH 8.0) was added and incubated for 30 min to quench any unreacted dye. The samples were then run on SEC (Superdex PC 3.2/30 column, 0.15 ml/min, GE Healthcare, Piscataway, NJ) to purify out the labeled NLP from unreacted dye. AF488-labeled NLP, CpG:NLP and MPLA:NLP were incubated with cells for 2 h at 37 °C and subsequently analyzed by flow cytometry. Flow cytometry was performed using a FACSCalibur (BD Biosciences) and data were analyzed using FlowJo version 9.5.3 software (Tree Star). For intracellular localization experiments, J774 cells were incubated with 50 nM LysoTracker Red DND-99 (Invitrogen) or Mitotracker Red (Invitrogen) for 2 h at 37 °C. After incubation, the cells were rinsed 3 times with fresh media. Cells were then incubated with AF488 labeled NLP constructs for 24 h at 37 °C. Bright field and fluorescent images of the dual labeled cells were then acquired using an Axiovert 200M microscope (Zeiss, Minneapolis, MN) in the multiple channel mode, which was equipped with a Photometric CoolSNAP HQ CCD camera (Photometrics, Tucson, AZ). The AF488 labeled NLPs were imaged using a 450–490 nm excitation filter and a 505 nm emission filter and the LysoTracker or MitoTracker dyes were imaged using a 510 – 560 excitation filter and 590 emission filter. Images were analyzed and processed using the AxioVision Rel 4.6 software.

2.10. Quantification of cytokine/chemokine secretion

Serum cytokine levels were assessed 4 h post-IP injection with the indicated concentrations of NLP, CpG:NLP, MPLA:NLP, free MPLA, free CpG, or PBS vehicle control. Capture ELISAs were performed to quantify IL-6, TNF-α, IL-1β, MIP-1α, and RANTES production. TNF-α, IL-1β, MIP-1α and RANTES were quantified using DuoSet kits (R&D Systems) according to the manufacturer's instructions. IL-6 was quantified using a purified/biotinylated antibody pair (clones MP5-20F3 and MP5-32C11; BD Biosciences). All ELISAs were detected using Streptavidin-HRP (BD Biosciences) and SureBlue Reserve TMB (3,3′,5,5′ – Tetramethylbenzidine) substrate (KPL Inc., Gaithersburg, MD).

2.11. Isolation of splenic RNA and quantitative RT-PCR

NLP (equivalent apoE422k dose as the 5 μg MPLA:NLP complexes, *ca.* 75 μg), CpG:NLP or CpG (40 μg), MPLA:NLP or MPLA (5 μg), or PBS were injected IP into mice (4 per group). Spleens were collected 30 min and 2 h post-injection and immediately placed in RNAlater stabilization solution (Qiagen) to preserve RNA integrity. RNA was subsequently purified from stabilized spleens using RNeasy Microarray Tissue Mini Kits (Qiagen), and RNA from two spleens was pooled (0.25 μg each) in order to generate two cDNA samples per experimental condition using RT^2 First Strand Synthesis kits (Qiagen) according to manufacturer's instructions. Real-time quantitative RT-PCR analysis of the samples was carried out using the mouse antibacterial response PCR array (SABiosciences) on an ABI Prism 7000 sequence detector (Applied Biosystems). Expression levels of target genes are reported as the average fold change calculated from 2 independent arrays as compared to expression levels in PBS control spleens. Data were analyzed using SABioscience's online analysis software available at http://pcrdataanalysis.sabiosciences.com/pcr/arrayanalysis.php.

2.12. Flow cytometric analysis of activation markers on splenic APCs

NLP (equivalent apoE422k dose as the 10 μg MPLA:NLP), CpG:NLP or CpG (40 μg), MPLA:NLP or MPLA (10 μg), or PBS were injected IP into mice and spleens were harvested 24 h post-injection. Single cell suspensions of splenocytes were generated by injecting each spleen with 200–500 μl of a solution of Liberase (1.67 U/ml, Roche) and DNAse I (0.2 mg/ml, Roche) in RPMI + 10% FBS and incubated for 30 min at 37 °C before manual dissociation through 70 μm filters. Red blood cells were lysed by incubation in 1 ml ACK lysis buffer (Life technologies) for 5 min at room temperature. 2×10^6 cells per stain were incubated in 100 μl PBS + 2% FBS with Fc block (1:100 dilution, clone 2.4G2; BD Biosciences) along with the following antibodies (all from BD Biosciences unless otherwise noted): CD11b-APC (1:250 dilution, clone M1/70), CD11c-PE (1:500 dilution, clone HL3), CD80-FITC (1:200 dilution, clone 16-10A1), CD86-FITC (1:200 dilution, clone GL1), CD40-FITC (1:200 dilution, clone 3/23), or I-A/I-E Alexa Fluor 488 (1:2000 dilution, clone M5/114.15.2, BioLegend) for 30 min on ice. 7AAD (2 μl per sample, BD Biosciences) was added 5 min prior to sample acquisition for dead cell exclusion. Flow cytometry was performed using a FACSCalibur and data were analyzed using FlowJo software.

2.13. In vivo and ex vivo analyses of CpG uptake

For *in vivo* analysis of CpG uptake, NLPs were assembled with a CpG that had been modified to include a cholesterol moiety at the 5′ end and a Quasar 670 molecule at the 3′ end (custom ordered Biosearch Technologies, Novato, CA). Mice were injected IP with 40 μg CpG-Quasar 670:NLP or free CpG-Quasar 670 and spleens were harvested at the indicated time points. A single cell suspension of splenocytes was obtained and stained for flow cytometric analysis as described above. 2×10^6 cells per stain were incubated in 100 μl PBS +2% FBS with Fc block (1:100) along with the following antibodies (all from BD Biosciences): CD11c-FITC (1:200 dilution, clone HL3), CD11b-PE (1:2000 dilution, clone M1/70) and CD45R-PE (1:1500 dilution, clone RA3-6B2). 7AAD (2 μl per sample) was added 5 min prior to sample acquisition for dead cell exclusion. Cell populations were defined as macrophages ($CD11b^+$ $CD11c^-$), conventional dendritic cells (cDCs, $CD11c^+$ $CD45R^-$) and plasmacytoid dendritic cells (pDCs, $CD11c^+$ $CD45R^+$). Flow cytometry was performed using a FACSCalibur and data were analyzed using FlowJo software. For *ex vivo* analysis, single cell suspensions of splenoctyes were purified into $CD11b^+$ and $CD11c^+$ populations using MACS beads (Miltenyi biotech) sorting according to the manufacturer's instructions. Purified cells (5×10^5) were incubated with 1 μg/ml CpG-Quasar 670:NLP or CpG-Quasar 670 in 12-well plates for 1 h then analyzed for CpG-Quasar 670 uptake by flow cytometry. Flow cytometry was performed using a FACSCalibur and data were analyzed using FlowJo software.

2.14. Intracellular cytokine expression in human dendritic cells

Intracellular cytokine expression was assessed using methods similar to those previously described [48]. Whole blood was collected from healthy human donors through BD Biosciences' internal donor program. Peripheral blood mononuclear cells (PMBCs) were isolated from blood using BD Vacutainer Cell Preparation Tubes (BD Biosciences), and 1.5×10^6–2.5×10^6 cells were activated with the indicated

concentrations of CpG:NLP, MPLA:NLP, CpG or MPLA in RPMI + 10% FBS at 37 °C for 2 h. Brefeldin A (BD Biosciences) was added to a final concentration of 10 μg/ml and cells incubated for an additional 2 h at 37 °C. Cells were then treated with 2 mM EDTA for 15 min at room temperature and then placed in an 18 °C water bath overnight. For cell surface marker detection (all antibodies from BD Biosciences), cells were incubated for 30 min at room temperature with the following antibodies: Lin 1-FITC, CD123-PerCP-Cy 5.5 and CD11c-APC using recommended concentrations. Cells were then fixed and permeabilized using BD Cytofix/Cytoperm solution (BD Biosciences) for 30 min at room temperature. The cells were then incubated with the following antibodies for intracellular protein detection: IFN-α-PE, TNF-α-PE-Cy7 and HLA-DR APC-H7 at the recommended concentrations. Samples were acquired using a BD FACSCanto (BD Biosciences) and data analyzed using FlowJo software.

2.15. Influenza challenge

Mice were treated with 10 μg CpG:NLP, NLP, CpG, or PBS intranasally. After 24 h, mice were anesthetized by IP injection with tribromoethanol at a dose of 200–250 μl per mouse. Mice were infected intranasally with 5×10^3 EID_{50} of A/PR/8/34 (generously provided by Andrew Caton, The Wistar Institute) in 30 μl phosphate-buffered saline (PBS). Mice were weighed daily for weight loss. Mice were euthanized upon losing 30% of their body weight during the time course.

3. Results

3.1. Assembly and characterization of agonist:NLP complexes

MPLA and CpG were incorporated into NLPs as outlined in Fig. 1 (A and D) to generate MPLA:NLP and CpG:NLP, respectively. To assess the incorporation of MPLA into the NLP platform, MPLA was added to the assembly reaction at MPLA to NLP molar ratios varying from 0.8 to 6.6. Incorporation into the NLPs was monitored by HPLC using an evaporative light scattering detector. HPLC chromatograms of the MPLA peak at increasing MPLA to NLP ratios are shown in Fig. 1B. As expected, an increase in the MPLA peak intensity was observed with an increase in the MPLA to NLP ratio. However, this increase was not linear, indicating that at higher ratios a significant proportion of the MPLA added to the assembly did not incorporate into NLPs. To quantify this effect, the final MPLA to NLP ratios in the purified MPLA:NLP constructs were plotted as a function of the

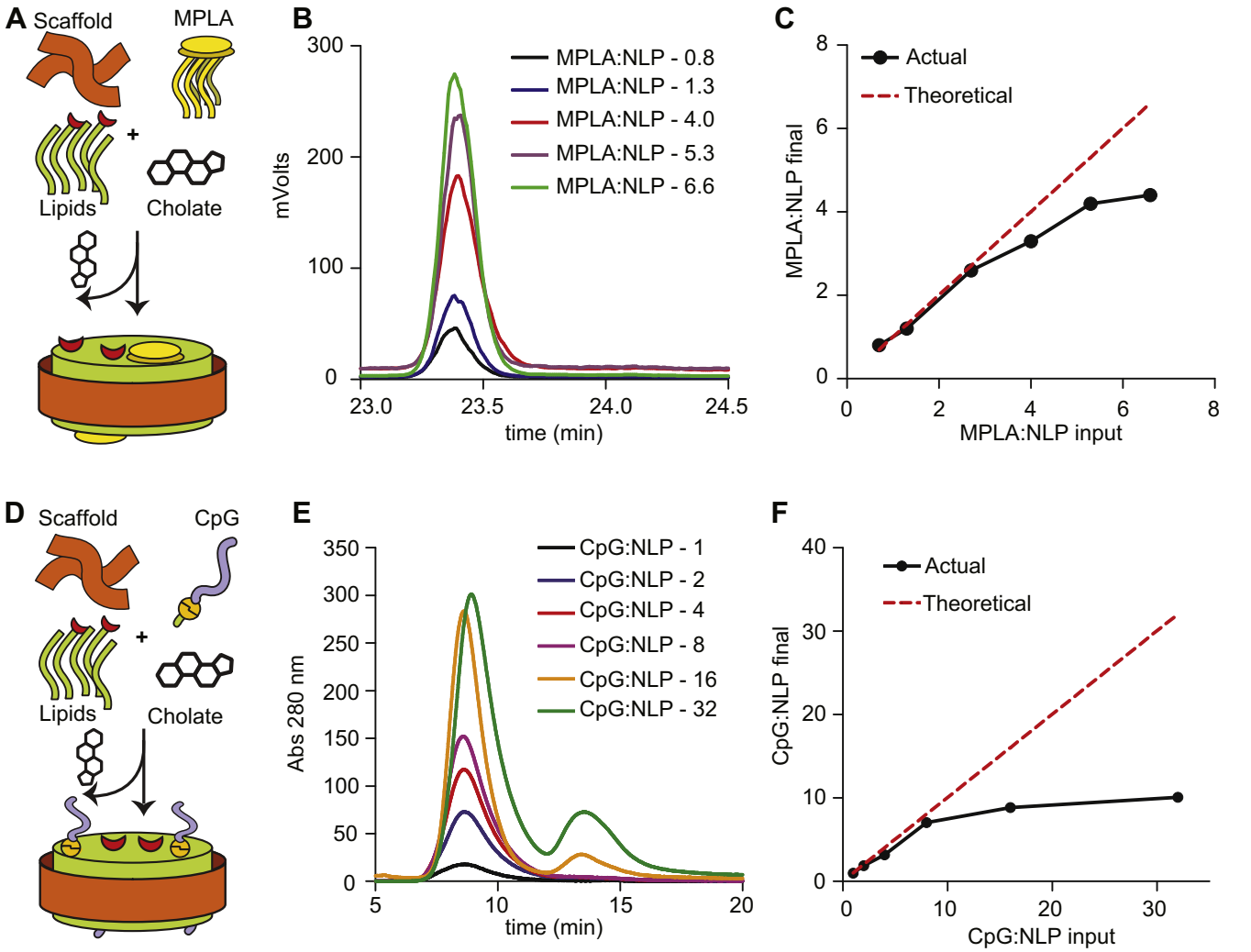

Fig. 1. MPLA and CpG are readily incorporated into the NLP. (A) Schematic of the self-assembly process used for incorporation of MPLA. (B) Purified MPLA:NLPs were assessed by reverse phase HPLC, and the chromatogram region corresponding to MPLA elution (t_R = 23.35 min) is shown. (C) Analysis of MPLA incorporation into the NLP as a function of increasing initial MPLA-to-NLP assembly ratios. A strong linear correlation between the input and final MPLA-to-NLP ratios was observed up to ~3 MPLA molecules per NLP. At higher ratios, MPLA incorporation was less efficient. (D) Schematic of the self-assembly process used for incorporation of CpG. (E) CpG:NLP assemblies prepared with increasing amounts of CpG were assessed by SEC. At increasing CpG incorporation ratios, a decrease in the NLP peak elution time (from t_R = 9 min to t_R = 8 min) was observed, coupled with an increase in peak absorbance intensity. These are both characteristics of successful CpG incorporation. Unincorporated CpG is observed at the highest CpG ratios (tR = 13.5). (F) Analysis of CpG incorporation into the NLP at increasing initial CpG-to-NLP ratios. A strong correlation between the input and final CpG-to-NLP ratios was observed up to ~9 CpG molecules per NLP. At higher CpG ratios, significant amounts of CpG were not incorporated into the NLP. CpGs were quantified using the Quant-iT OliGreen ssDNA quantification reagent.

initial MPLA to NLP ratio used in the assembly reaction (MPLA:NLP input, Fig. 1C). The experimental values closely follow the theoretical plot (i.e. all MPLA in the reaction is incorporated into the NLP) up to a mole ratio of ~3. At higher ratios, the actual incorporation values deviate from the theoretical values, indicating a decrease in the efficiency of MPLA incorporation at higher ratios. Thus, for all subsequent experiments NLPs were assembled at an MPLA to NLP molar ratio of 3.

Similar titration assembly reactions were performed with CpG and incorporation was evaluated by size exclusion chromatography (SEC) (Fig. 1E). NLPs were assembled at CpG to NLP molar ratios ranging from 1 to 32. Since CpG (retention time (t_R) 13.5 min) is significantly smaller than the NLP (t_R 9 min), unincorporated CpG was readily resolved from the NLP by SEC. In the SEC analysis, a decrease in the NLP t_R (shifted from 9 min down to 8 min) and an increase in the peak intensity was observed, indicative of CpG incorporation. The shift in retention time was expected since incorporation of many larger compounds into the NLP, including CpG, should increase the overall stokes diameter of the NLP [44]. In addition, the increase in absorbance at 280 nm was expected with CpG incorporation due to the inherent absorbance of CpG at 280 nm. Therefore, these two trends indicate successful incorporation of CpG. At CpG to NLP ratios of 16 and higher, a peak corresponding to unincorporated CpG was observed (t_R 13.5 min) in addition to the CpG:NLP construct. To quantitatively measure incorporation efficiency, CpG:NLPs were purified by SEC. The CpG to NLP ratios in the SEC-purified constructs were plotted as a function of the initial CpG to NLP ratio that was used in the assembly reaction (CpG:NLP input, Fig. 1F). Based on this analysis, the incorporated CpG in the assembled particle tracked very closely with the theoretical value up to a ratio of approximately 8 (i.e. all CpG added to the assembly was incorporated into the NLP). The trend deviated substantially from the theoretical values at ratios higher than 10, and very little additional CpG was incorporated in the NLP at CpG to NLP input ratios above 20. Thus, to maximize CpG incorporation into the NLP while minimizing loss of unincorporated CpG, CpG:NLPs were assembled at a CpG to NLP ratio of 20 for all subsequent experiments. These combined results demonstrate successful incorporation of both CpG and MPLA into the NLP and accurate quantitation of CpG and MPLA concentrations.

3.2. Immunostimulatory properties of agonist:NLP complexes

To evaluate the interactions between NLPs and immune cells, we first assessed the ability of mouse macrophages to internalize the NLP complexes. NLPs, MPLA:NLPs and CpG:NLPs (fluorescently labeled with AF488) at a concentration of 1 μg/ml, based on apoE422k scaffold protein concentration, were incubated with mouse J774 cells and primary peritoneal macrophages (pMP) for 2 h and uptake of the particles was quantified by flow cytometry.

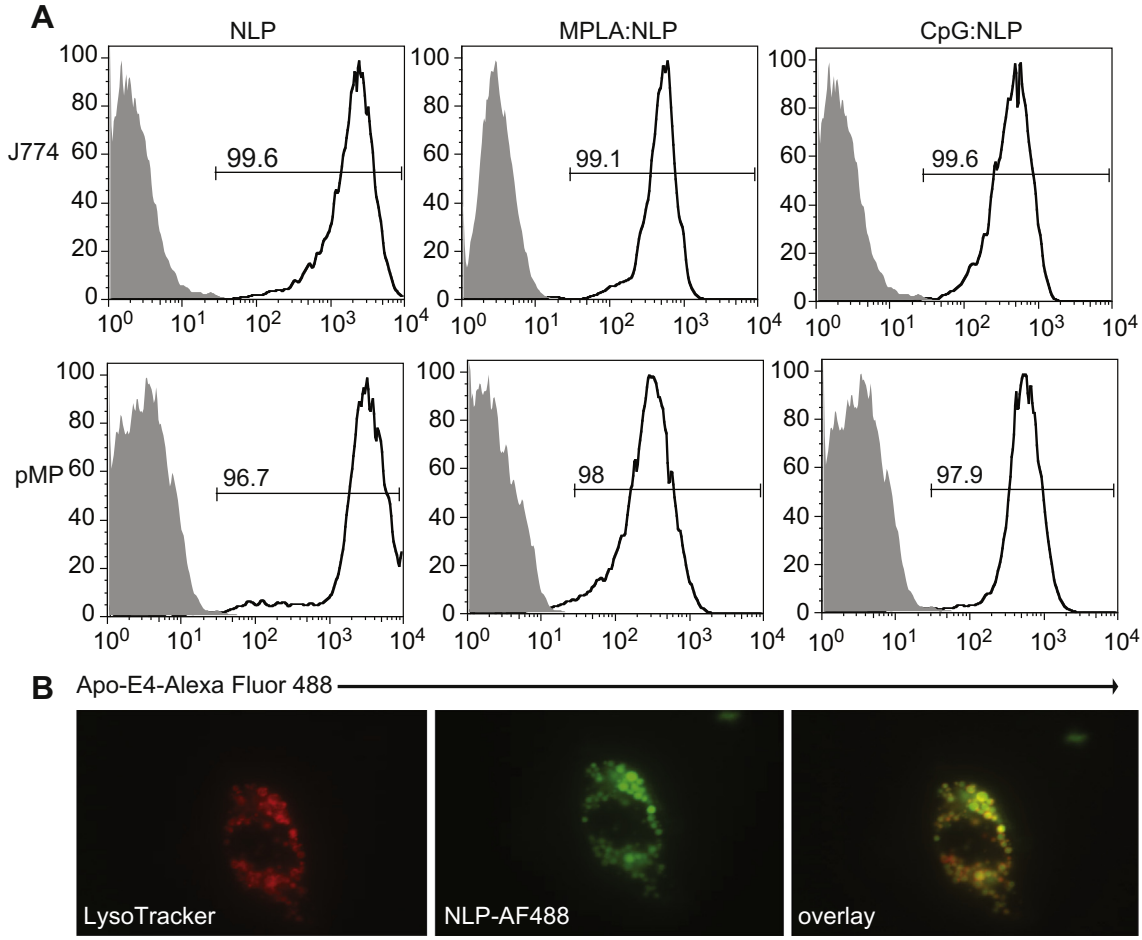

Fig 2. NLPs are rapidly internalized by mouse macrophages *in vitro*. (A) Mouse macrophage-like cell line J774A.1 (J774) or primary peritoneal macrophages (pMP) were incubated for 2 h with 1 μg (based on apoE422k concentration) of the indicated NLPs assembled with AF488-labeled apoE422k scaffold protein, then analyzed by flow cytometry. The solid gray histograms indicate control cells not incubated with NLPs. Numbers in the plots indicate the percentage of cells positive for AF488 in a representative experiment performed three times. (B) J774 macrophages were incubated with AF488-labeled NLPs with or without LysoTracker, and analyzed at 24 h by fluorescence microscopy. Images were taken from a representative experiment performed in triplicate.

NLP constructs were rapidly internalized, where >99% of J774 cells (top panel) and >96% of pMP (bottom panel) were positive for AF488 fluorescence (Fig. 2A). This rapid internalization of NLPs was not cargo dependent since all constructs were internalized similarly.

Because MPLA and CpG interact with cell-surface and endosomal TLRs, respectively, we next assessed the subcellular localization of NLPs upon internalization. J774 cells were pre-treated with LysoTracker dye for 1 h prior to addition of AF488-labeled NLPs and analyzed 24 h later by confocal microscopy. AF488-labeled NLPs co-localized with the LysoTracker dye, indicating that the particles were trafficked to lysosomes (Fig. 2B). Similar experiments were performed using MitoTracker dye, where no co-localization of AF488-labeled NLPs with MitoTracker was observed in the mitochondria (data not shown). Taken together, these results demonstrate that NLP constructs are rapidly internalized by mouse macrophages and trafficked to lysosomes for degradation.

Next, we investigated the ability of NLP constructs to activate mouse macrophages *in vitro*. CpG:NLPs and MPLA:NLPs were compared to free CpG and MPLA at various concentrations for their ability to elicit cytokine secretion by J774 cells. As a control, empty NLPs without conjugated agonists were included at equivalent doses (estimated based on apoE422k scaffold protein concentration) to both CpG:NLP and MPLA:NLP constructs. CpG:NLP and MPLA:NLP constructs elicited higher levels of IL-6, TNF-α and RANTES compared with equivalent doses of free CpG and MPLA (Fig. 3A and B). In order to assess whether CpG:NLPs and MPLA:NLPs elicited a similar pattern of enhanced cytokine secretion in a more relevant *in vitro* model, pMP were stimulated with NLP, CpG:NLP, MPLA:NLP, free CpG, or free MPLA. Similar to what was observed in J774 cells, conjugation of CpG or MPLA to NLPs significantly enhanced their immunostimulatory abilities compared with the equivalent dose of free CpG or free MPLA (Fig. 3C and D). Interestingly, empty NLPs elicited low levels of IL-6,

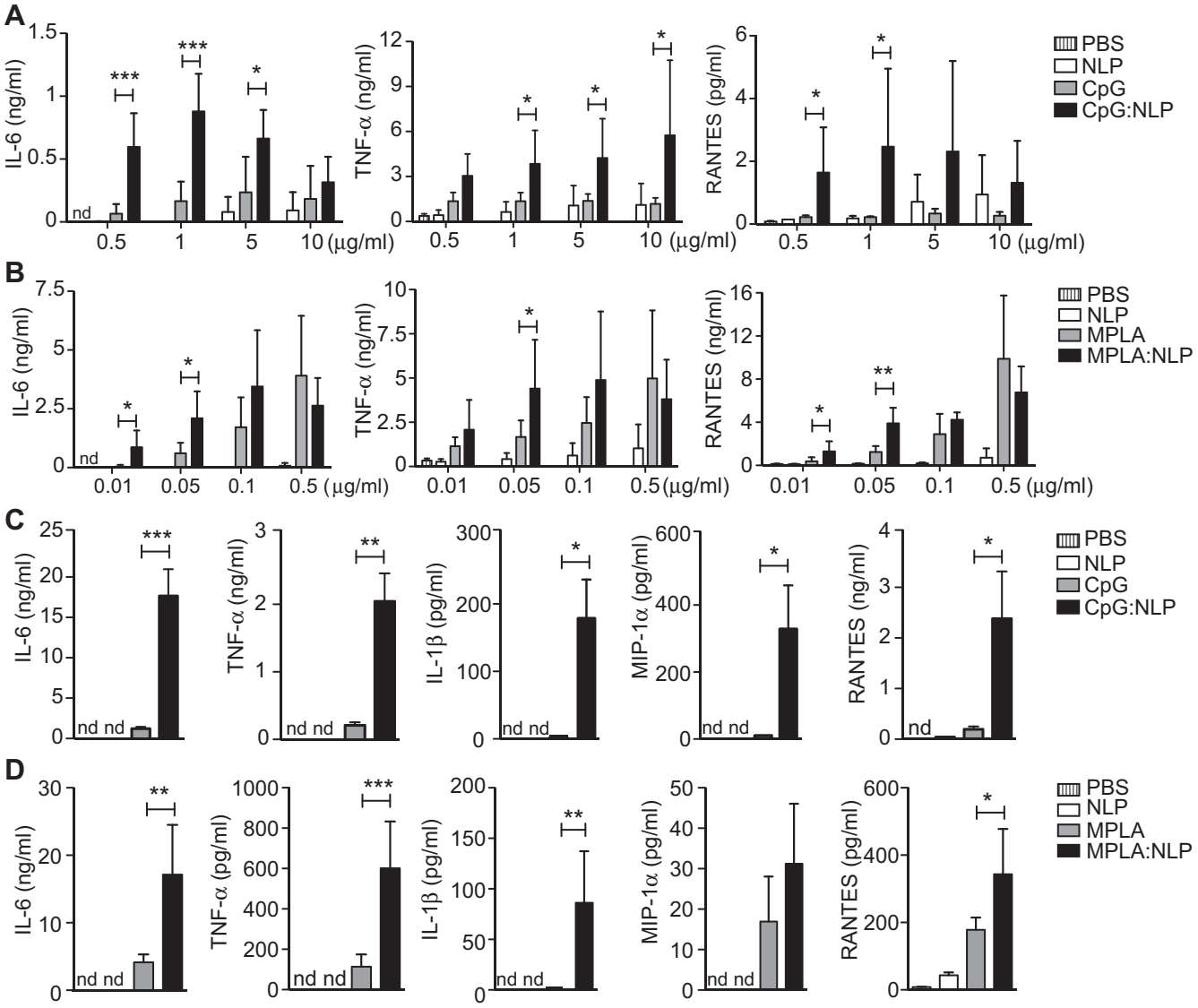

Fig. 3. Conjugation of TLR agonists to NLPs enhances cytokine production by mouse macrophages *in vitro*. J774 cells were stimulated with the indicated concentrations of CpG (A) or MPLA (B), either as free agonists or conjugated to NLPs. As a control, NLPs with no agonists were included at the equivalent apoE422k scaffold protein concentrations as agonist:NLP constructs (A–D). Supernatants were collected 24 h later and assayed for the indicated cytokines by ELISA. Primary mouse peritoneal macrophages were stimulated with 1 μg/ml CpG (C) or 0.05 μg/ml MPLA (D) and supernatants were collected 24 h later and assayed for cytokines as above. Results are represented as mean values of triplicate experiments with standard deviation error bars. nd = not detected. $^{*}p < 0.05$, $^{**}p < 0.01$, $^{***}p < 0.001$ (Student's *t* test).

TNF-α, and RANTES in J774 cells in a dose-dependent fashion, and small but detectable levels of RANTES in pMP (Fig. 3A–D). Taken together, these data demonstrate that conjugation to NLPs enhanced the immunostimulatory abilities of CpG and MPLA *in vitro* and suggest that empty NLPs elicit a weak immunostimulatory response.

We next addressed whether NLP conjugation also enhanced immunostimulation by CpG and MPLA *in vivo*. NLP, CpG:NLP, MPLA:NLP, free CpG, and free MPLA were injected IP into mice at various doses and serum was harvested 4 h later to quantify cytokine levels by ELISA. Significantly higher levels of serum IL-6, TNF-α, MIP-1α and RANTES were induced by CpG:NLP administration compared to free CpG at the 40 μg dose. Similarly, MPLA:NLP constructs elicited significantly higher levels of IL-6, TNF-α, MIP-1α and RANTES cytokine levels compared with free MPLA at every dose tested (Fig. 4B). As was observed *in vitro*, empty NLPs elicited low levels of cytokines in a dose dependent manner *in vivo*. (Fig. 4B). These data demonstrate that conjugation to NLPs enhances the immunostimulatory abilities of CpG and MPLA both *in vitro* and *in vivo*.

To further characterize the extent to which NLP conjugation enhances stimulation by CpG and MPLA *in vivo*, we assessed activation at the cellular level by quantifying cell surface expression of proteins involved in antigen presentation and costimulation on macrophages and dendritic cells. Mice were injected IP with NLP, CpG:NLP, MPLA:NLP, free CpG, or free MPLA, and spleens were harvested 24 h post-injection. Splenocytes were isolated and stained for cell surface markers to identify macrophages ($CD11b^+$ $CD11c^-$) and dendritic cells ($CD11c^+$), as well as the activation markers MHC class II (I-A/I-E), CD80, and CD40 on the surface of macrophages (Fig. 4C) and CD86, CD80, and CD40 on the surface of dendritic cells (Fig. 4D). The expression levels of all activation markers on both cell types were significantly higher following injection with CpG:NLP or MPLA:NLP relative to free agonists (Fig. 4C and D). Comprehensively,

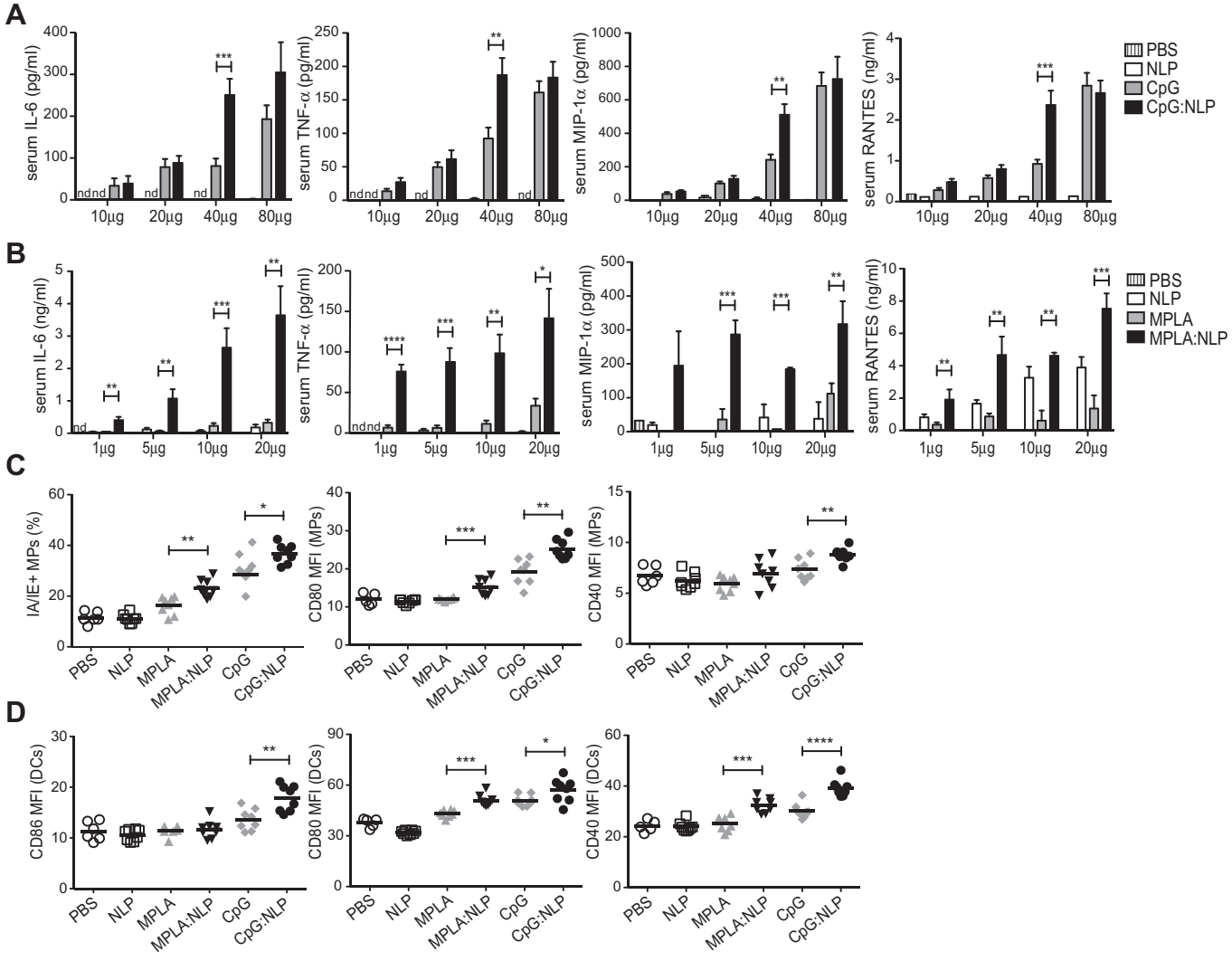

Fig. 4. Conjugation of TLR agonists to NLPs enhances innate immune responses *in vivo*. Male BALB/c mice were injected IP with the indicated dose of CpG (A) or MPLA (B), either free or conjugated to NLPs, or NLP at the equivalent apoE422k protein concentration. Serum was collected 4 h post-injection and assayed for the indicated cytokines by specific capture ELISAs. Results are represented as mean values calculated from 10 mice, conducted as 2 independent experiments of 5 mice each, with standard deviation error bars. Male BALB/c mice were injected IP with 10 μg MPLA (C) or 40 μg CpG (D), either free or conjugated to NLPs, or NLP at the equivalent apoE422k protein concentration. Splenocytes were harvested 24 h later and levels of expression of the indicated surface markers assessed by flow cytometry on (C) macrophages ($CD11b^+$ $CD11c^-$) and (D) dendritic cells ($CD11c^+$). Results are represented as mean values calculated from 8 mice per group, conducted as 2 independent experiments of 5 and 3 mice per group, with standard deviation error bars. $^*p < 0.05$, $^{**}p < 0.01$, $^{***}p < 0.001$, $^{****}p < 0.0001$ (Student's *t* test). nd = not detected.

A

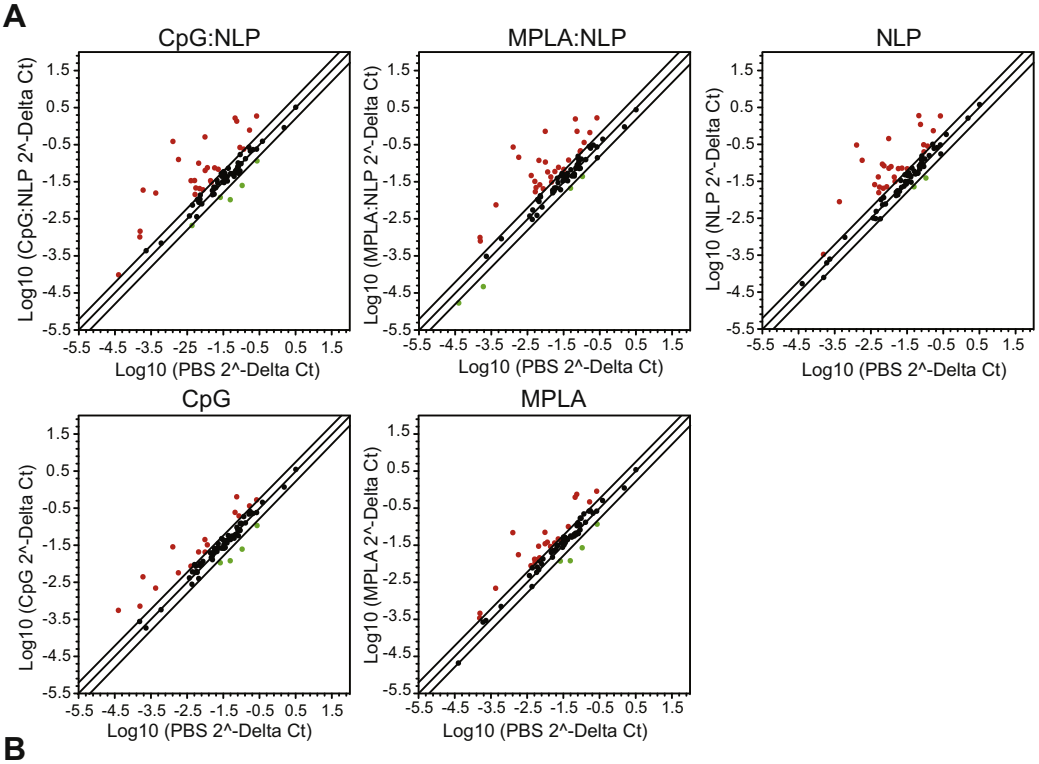

B

Fold expression (versus PBS control)

	Gene	Description	Treatment				
			CpG	MPLA	NLP	MPLA:N	CpG:N
TLR/NLR signaling	Birc3	Baculoviral IAP repeat-containing 3					
	Cd14	CD14 antigen					
	Lpb	Lipopolysaccharide binding protein					
	Ly96	Lymphocyte antigen 96					
	Irak3	Interleukin-1 receptor-associated kinase 3					
	Mefv	Mediterranean fever					
	Myd88	Myeloid differentiation primary response gene 88					
	Nlrp3	NLR family, pyrin domain containing 3					
	Nfkb1	NFκB 1, p105					
	Nfkbia	NFκB inhibitor, alpha					
	Nod2	Nucleotide-binding oligomerization domain containing 2					
	Rela	V-rel reticuloendotheliosis viral oncogene homolog A					
	Ripk2	Receptor (TNFRSF)-interacting serine-threonine kinase 2					
	Ticam2	Toll-like receptor adaptor molecule 2					
	Tlr2	Toll-like receptor 2					
cytokines/chemokines	Ccl3	Chemokine (C-C motif) ligand 3					
	Ccl4	Chemokine (C-C motif) ligand 4					
	Ccl5	Chemokine (C-C motif) ligand 5					
	Cxcl1	Chemokine (C-X-C motif) ligand 1					
	Cxcl3	Chemokine (C-X-C motif) ligand 3					
	Il12b	Interleukin 12B					
	Il18	Interleukin 18					
	Il1b	Interleukin 1 beta					
	Il6	Interleukin 6					
	Tnf	Tumor necrosis factor					
other inflammatory	Akt1	Thymoma viral proto-oncogene 1					
	Apcs	Serum amyloid P-component					
	Bpi	Bactericidal permeability increasing protein					
	Camp	Cathelicidin antimicrobial peptide					
	Crp	C-reactive protein, pentraxin-related					
	Ctsg	Cathepsin G					
	Dmbt1	Deleted in malignant brain tumors 1					
	Jun	Jun oncogene					
	Lcn2	Lipocalin 2					
	Ltf	Lactotransferrin					
	Mpo	Myeloperoxidase					
	Zbp1	Z-DNA binding protein 1					

Fold expression
> 100 fold increase
20–100 fold increase
5–20 fold increase
2–5 fold increase
< 2 fold change
2–5 fold decrease

these data demonstrate that agonist:NLP constructs elicit more robust innate immune responses *in vivo* than free agonists alone administered at equivalent doses.

3.3. Immunoregulatory gene expression in vivo

In order to understand the mechanism(s) underlying the ability of the NLP to augment the immunostimulatory profiles of CpG and MPLA *in vivo*, we investigated changes in gene expression elicited by NLP, CpG:NLP, MPLA:NLP, free CpG, or free MPLA treatment using quantitative RT-PCR pathway arrays. The mouse antibacterial response array (SABiosciences), which simultaneously measures the expression of 84 genes previously demonstrated to be involved in innate responses to bacterial infections, was used to analyze gene expression in the spleen 30 min and 2 h post-IP injection. Changes in gene expression were minimal after 30 min (data not shown). However, robust changes in the levels of gene expression in a number of key genes were detected (Fig. 5) after 2 h. Interestingly, scatterplot analysis indicated that the numbers of genes exhibiting at least a ±2-fold regulation were more similar among the NLP, CpG:NLP and MPLA:NLP groups than either CpG:NLP or MPLA:NLP with their corresponding free agonist controls (Fig. 5A). Furthermore, the magnitude of those changes was consistently much higher among the NLP, CpG:NLP and MPLA:NLP groups than either free CpG or MPLA. The levels of expression of those genes exhibiting at least a ±2-fold regulation are summarized in Fig. 5B (for a full summary of the changes in gene expression for all 84 genes, see Supplemental Table 1). Both CpG:NLP and MPLA:NLP induced much higher levels of expression of a number of genes than either CpG or MPLA alone (Fig. 5B). Included in this set are many genes encoding cytokines and chemokines, as well as several genes involved in TLR and NF-κB signaling pathways. Surprisingly, the NLP alone also induced high levels of expression of many of the same genes, in some cases equal or almost equal to levels induced by either CpG:NLP or MPLA:NLP (Fig. 5B; Supplemental Table 1). Indeed, based on the patterns of gene expression, it appears that the majority of the gene upregulation induced by CpG:NLP and MPLA:NLP could be attributed to the NLP rather than CpG or MPLA. These data suggest that the NLP itself is immunostimulatory at the doses examined in these studies and may explain, in part, the ability of the NLP to augment the immunostimulatory profiles of CpG and MPLA *in vivo*.

3.4. Uptake and trafficking of CpG:NLPs

To investigate changes in the biodistribution and trafficking of agonists associated with NLP conjugation, we used flow cytometry to quantify the amount of fluorescently-labeled CpG:NLP and CpG in the spleen following IP injection. CpG-Quasar 670:NLP and free CpG-Quasar 670 were injected into mice and spleens were harvested 4, 24, 48 and 72 h post-injection and analyzed for the presence of CpG-Quasar 670 (Fig. 6). Conjugation of CpG-Quasar 670 to the NLP resulted in a significant increase in the percentage of splenocytes that were Quasar 670 positive by 4 h (average 60% versus 35%, Fig. 6A). Increases in the percentage of CpG positive splenocytes with NLP conjugation were even more dramatic at later time points, with greater than 3-fold more splenocytes exhibiting Quasar 670 fluorescence at 24, 48 and 72 h post-injection when the labeled CpG was conjugated to the NLP. Uptake by specific cell types was determined by antibody staining (Fig. 6B–D). Uptake by macrophages and dendritic cells was similar at the 4-h time point, but significant differences emerged at later time points (Fig. 6B–D). These data suggest that conjugation to NLPs may enhance trafficking of CpG to the spleen, retention of CpG at later time points, and/or uptake of CpG on a per cell basis, or a combination of all three scenarios. Enhancement of uptake by conjugation to NLPs was confirmed using purified splenocyte populations *ex vivo*. Splenocytes were sorted into $CD11c^+$ and $CD11b^+$ populations and incubated with CpG-Quasar 670, either free or conjugated to NLPs, for 1 h and then analyzed by flow cytometry. NLP conjugation resulted in significant enhancement in the amount of CpG-Quasar 670 taken up by both cell populations, as measured by mean fluorescence intensity of the Quasar 670 signal (Fig. 6E and F). While further experiments are needed to fully elaborate the mechanisms by which NLPs may alter biodistribution and retention of agonists *in vivo*, these results indicate that conjugation to the NLP enhances uptake of CpG into cells. It is worth noting that these experiments were only performed with CpG:NLPs because MPLA is not amenable to labeling with a fluorescent dye; however, we hypothesize that a similar trend would likely be observed for MPLA:NLPs as this effect was due to delivery via the NLP platform.

3.5. Activation of primary human DCs

In order to assess the translatability of our results to humans, we investigated the ability of the NLP to enhance stimulation by CpG and MPLA in primary human dendritic cells. PBMCs collected from two healthy human donors were incubated with CpG:NLP, MPLA:NLP, free CpG, or free MPLA at various doses for 4 h and subsequently analyzed to quantify intracellular cytokine levels by flow cytometry. The gating scheme defining myeloid and plasmacytoid dendritic cells (mDCs and pDCs, respectively) is detailed in Fig. 7A. CpG:NLP stimulated significantly higher frequencies of IFN-α and TNF-α–producing pDCs compared with free CpG across the titration range (Fig. 7B). Significantly higher frequencies of TNF-α–producing mDCs were also observed in response to MPLA:NLP compared with free MPLA across the titration range (Fig. 7C). These results suggest that conjugation to NLPs enhances innate immune responses not only in murine cells, but in human cells as well, indicating the potential for clinical translatability of the NLP platform as an innate immune modulator. Importantly, comparison of innate immune responses to TLR agonists across different species allows for a more thorough understanding of species-specific sensitivities to TLR stimulation.

3.6. Influenza challenge

As proof of principle, the efficacy of agonist:NLP constructs at protecting against pathogen challenge was assessed using a mouse model of influenza. CpG:NLPs were selected for the challenge studies as prophylactic intranasal (IN) administration of CpG has

Fig. 5. NLP constructs induce robust changes in splenic gene expression *in vivo*. Male BALB/c mice were injected IP with 40 μg CpG:NLP or CpG, 5 μg MPLA:NLP or MPLA, NLP at the equivalent apoE422k protein concentration to 5 μg MPLA:NLP, or PBS vehicle control. Gene expression profiles were determined by quantitative RT-PCR using the mouse antibacterial response array (SABiosciences). Each array was performed in duplicate using RNA pooled from 2 mice, representing RNA from a total of 4 mice per condition. (A) Scatter plots summarizing expression of all 84 genes included in the array. Red circles represent genes upregulated by more than 2 fold, black circles represent genes less than 2 fold up or down regulated, and green circles represent genes down regulated by more than 2 fold versus PBS control samples. Data are plotted as the log10 of 2ΔCt values normalized to housekeeping gene controls. (B) Table summarizing the expression levels of those genes that were up or down regulated by greater than 2 fold in at least one condition. Values were calculated as $2(-\Delta\Delta Ct)$, with ΔΔCt calculated as ΔCt (experimental sample) −ΔCt (PBS control). (For interpretation of the references to colour in this figure legend, the reader is referred to the web version of this article.)

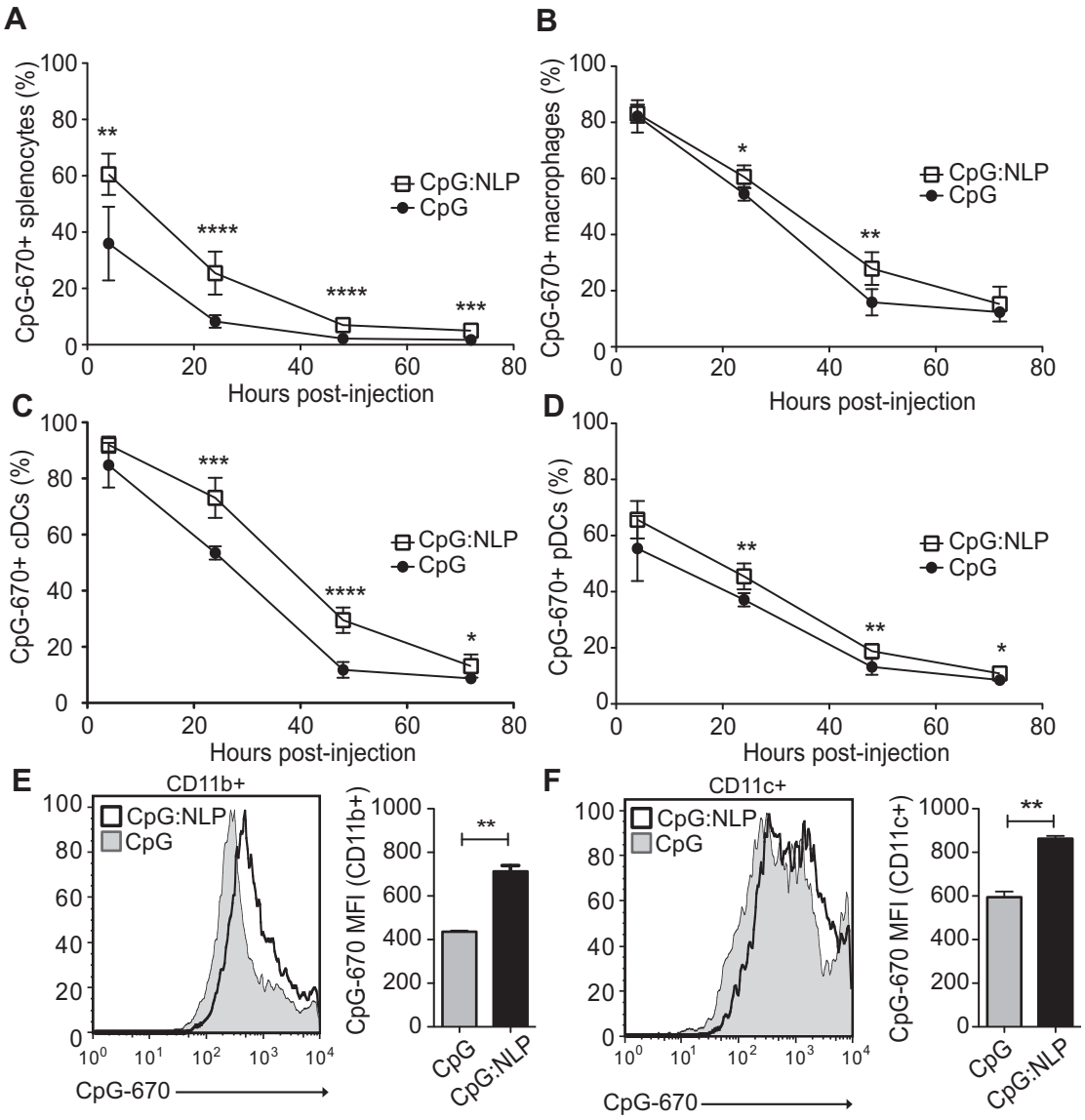

Fig. 6. NLPs enhance uptake of CpG by splenocytes. Male BALB/c mice were injected IP with 40 μg fluorescently-labeled CpG-Quasar 670 either free or conjugated to NLPs. Splenocytes were harvested at 4, 24, 48, and 72 h post-injection and analyzed by flow cytometry. Results are displayed as the % Quasar 670 positive total splenocytes (A), or as the % Quasar 670 positive of the indicated cell types as determined by antibody staining (B–D). Macrophages were defined as $CD11b^+$ $CD11c^-$. Conventional dendritic cells (cDCs) were defined as $CD11c^+$ $CD45R^-$. Plasmacytoid dendritic cells (pDCs) were defined as $CD11c^+$ $CD45R^+$. Results shown in (A) are averaged from two independent experiments and data points are mean values calculated from 10 mice with standard deviation error bars. Results in B-D are a representative of two independent experiments and data points are mean values calculated from 5 mice, with standard deviation error bars (E) and (F). NLPs enhance uptake of CpG by macrophages and DCs *in vitro*. Splenocytes were harvested from male BALB/c mice and MACS bead sorted into $CD11b^+$ (E) and $CD11c^+$ (F) populations. Purified cells were incubated with 1 μg/ml CpG-Quasar 670:NLP or CpG-Quasar 670 for 1 h *in vitro* then analyzed for Quasar 670 by flow cytometry. Histograms display representative samples of CpG-Quasar 670:NLP (black line) or CpG-Quasar 670 (shaded gray). Bar graphs display mean fluorescence intensity of the FL-4 channel calculated from duplicate samples of a representative experiment with standard deviation error bars. $^*p < 0.05$, $^{**}p < 0.01$, $^{***}p < 0.001$, $^{****}p < 0.0001$ (Student's *t* test).

previously been shown to confer partial protection in mice from lethal infection with the A/PR8/34 strain of influenza [23]. Mice were treated IN with 10 μg CpG:NLP, CpG, NLP or PBS 24 h prior to IN infection with a lethal dose of A/PR8/34 and weight loss was monitored each day post-infection. Only mice that received CpG:NLP prior to infection were afforded protection and survived the challenge out to day 14 (Fig. 8). Mice treated with NLP or free CpG exhibited progressive weight loss at a rate similar to PBS treated mice and were euthanized on day 7 post-infection. These data suggest that stimulation of innate immune responses by CpG:NLP provides protection from a lethal influenza challenge, underscoring the therapeutic potential of the NLP platform.

4. Discussion

In this study, we investigated the stimulatory properties of immunomodulatory complexes comprised of a nanolipoprotein particle platform and synthetic TLR agonists CpG and MPLA. We demonstrate that conjugation to NLPs enhances stimulation by both agonists *in vitro* and *in vivo* as measured by enhanced cytokine release, changes in immunoregulatory gene expression, and increased expression of key activation markers on the surface of APCs. We also demonstrated that conjugation to NLPs enhanced uptake of CpG by splenocytes, including both macrophages and DCs. Importantly, the effects of NLP conjugation were not specific to

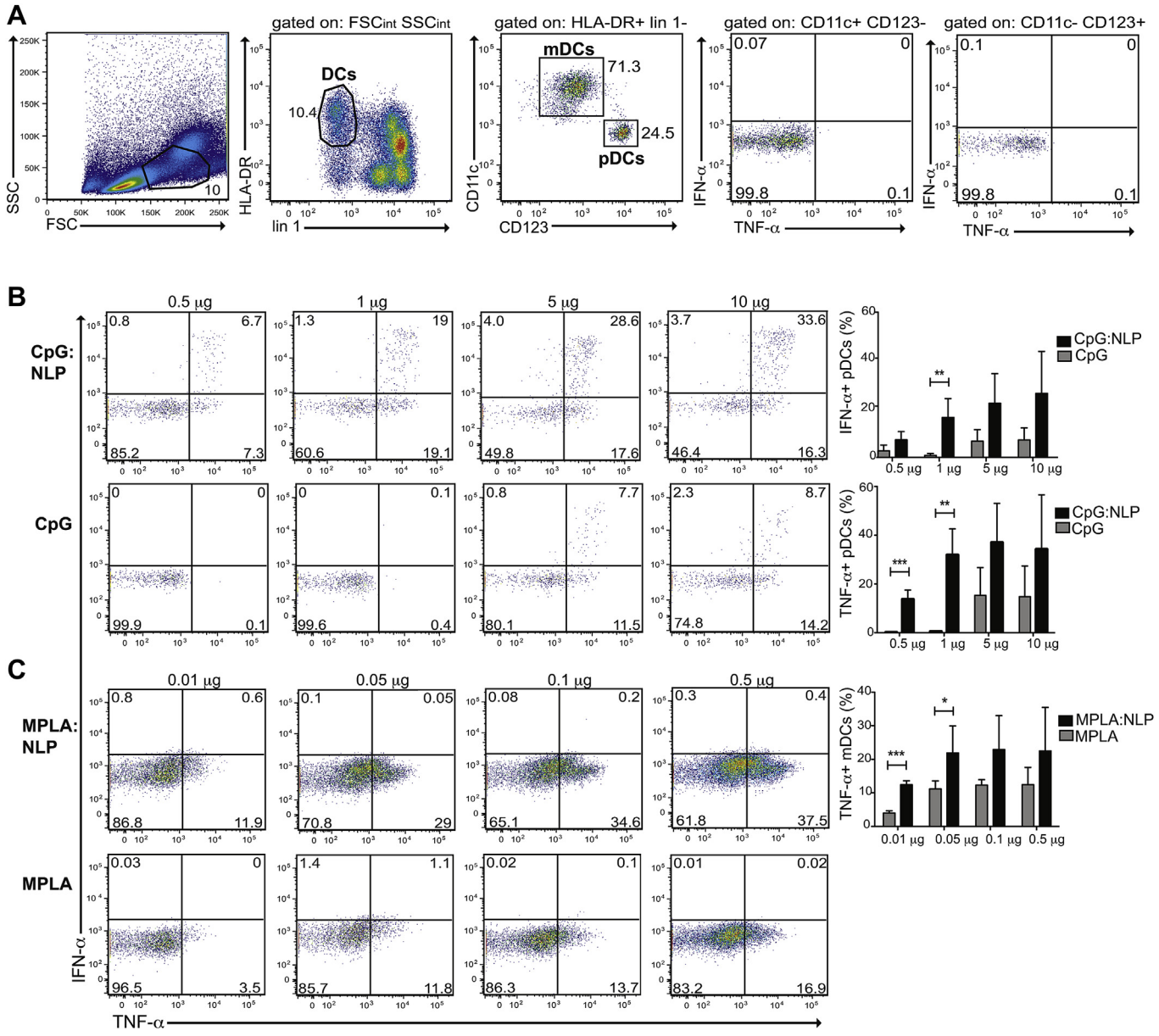

Fig. 7. Conjugation of TLR agonists to NLPs enhances cytokine production by human dendritic cells. PBMCs were purified from blood collected from healthy donors and stimulated for 4 h with CpG:NLP, MPLA:NLP, CpG or MPLA. Cells were then analyzed by flow cytometry for cytokine production. (A) Gating scheme that defines myeloid and plasmacytoid dendritic cells dendritic cells (mDCs and pDCs, respectively). Plots are gated successively from left to right. Dendritic cells are FSCint SSCint HLA-DR^{+} lin 1^{-}. Lin 1 is a cocktail containing antibodies against CD3, CD14, CD16, CD19, CD20, and CD56 to identify lymphocytes, monocytes, eosinophils, and neutrophils. HLA-DR is used to distinguish dendritic cells from basophils. mDCs and pDCs were distinguished by the expression of CD11c and CD123 respectively. The last two plots demonstrate the lack of IFN-α and TNF-α production by mDCs and pDCs, respectively, in a PBS control sample. (B) CpG:NLP stimulates more IFN-α and TNF-α-producing pDCs than CpG alone. Plots are representative data collected from one donor. Bar graphs represent the mean values of cytokine positive cells from 2 donors, performed in duplicate, with standard deviation error bars. (C) MPLA:NLP stimulates more TNF-α-producing mDCs than MPLA alone. Plots represent data collected from one donor. Bar graphs represent the mean values of cytokine positive cells from 2 donors, performed in duplicate, with standard deviation error bars. $^{*}p < 0.05$, $^{**}p < 0.01$, $^{***}p < 0.001$ (Student's t test).

the murine system as NLPs also enhanced stimulation of human DCs by both CpG and MPLA. Strikingly, mice that were treated prophylactically with CpG:NLP complexes survived a lethal influenza challenge, whereas mice that were treated with the equivalent amount of free CpG were afforded no protection.

These data have important implications for the development of host-based therapeutics targeting infectious disease. Pathogens labeled as having highest risk to national security and public safety (NIAID Category A pathogens) pose significant challenges, as viable therapeutic options are either not available or not optimal to treat naïve populations in the event of a widespread outbreak or deliberate release. In addition, there is a continual threat of the emergence of new pathogens against which no therapeutics exist, such as the coronaviruses responsible for the respiratory syndromes SARS and MERS [49], or of newly recombinant pathogenic strains of influenza yet to be encountered. Therefore, in the event of an intentional release or pandemic outbreak caused by such a pathogen, those individuals in the vicinity of the outbreak would be at risk of exposure with limited treatment options. An innate immune targeting therapeutic, such as the TLR agonist:NLP complexes described here, could be employed prophylactically in such an event to enable exposed individuals to build sufficient transient immunity to survive

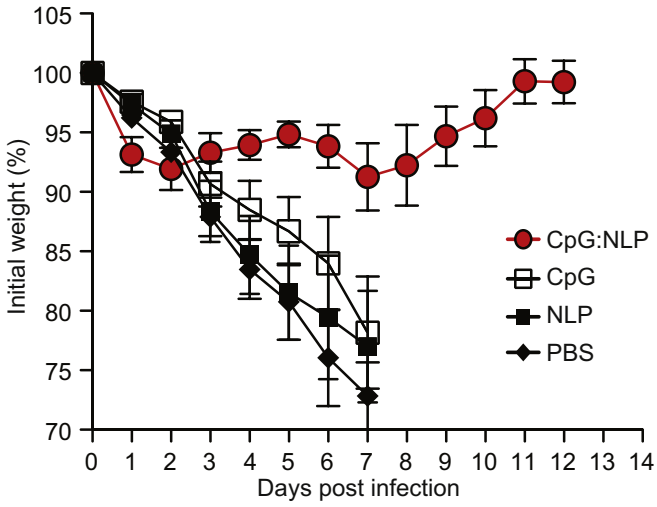

Fig. 8. CpG:NLP constructs protect against lethal influenza challenge. Female BALB/c mice were infected with a lethal dose of influenza virus A/PR/8/34 (5×10^3 EID_{50}). Mice were observed daily for weight loss and survival. Data shown are mean values +/− SEM of the percentage of initial weight for 6 mice in each group. Experiment shown is representative of 2 independent experiments.

what may otherwise be considered a lethal infection. There is precedent for targeting innate immunity as a prophylactic countermeasure against biothreat agents, as CpG has previously been shown to be protective in mice against *Francisella tularensis* and *Burkholderia pseudomallei* [17,24,25], and synthetic TLR4 agonists have been shown to be protective in mice against *F. tularensis* and *Y. pestis* [13–15]. However, the protection afforded in these studies was variable, with some demonstrating only marginally better survival than untreated control animals. In our study, mice that were pretreated with CpG as free agonists were not afforded any level of protection against influenza challenge whereas all mice that received CpG:NLP complexes survived infection. This suggests that administering TLR agonists complexed to a particle improves the therapeutic index of the agonists, and raises the intriguing possibility that the incomplete protection afforded in earlier studies may be improved upon by administration of TLR agonists-particulate complexes as opposed to free agonists alone.

While particulate delivery systems, mainly in the form of aluminum salts (alum), have been used for over a century, the mechanisms behind their enhancement of vaccine immunogenicity have only recently begun to be unraveled. To date, many varied types of synthetic micro and nanoparticles have been explored as vaccine platforms, and numerous studies have documented their wide range of effects on innate immune responses (extensively reviewed in Ref. [50]). Recent studies have demonstrated that alum in various forms, as well poly(lactic-co-glycolic acid) microparticles, can activate the NLRP3 inflammasome [35–37,51]. Reports have differed on the requirements and outcomes of inflammasome activation, and while the requirement for inflammasome activation in the subsequent induction of adaptive responses is unclear, activation of various aspects of innate immunity by particulate adjuvants is well established. Our data provide further evidence for nanoparticle-mediated activation of innate immune responses. Injection of animals with NLPs without agonists resulted in robust changes in the expression levels of genes encoding proteins involved in TLR/NLR signaling, cytokine and chemokine signaling, as well as other innate immune pathways (Fig. 5), suggesting the particle itself is immunostimulatory. While we did not look at activation of the inflammasome directly, genes related to inflammasome activation were upregulated following NLP injection, including Il1b and Nlrp3 (Fig. 5B). Interestingly, another recent study demonstrated that *in vitro* treatment of DCs with poly(γ-glutamic acid) particles induced expression of many genes involved in TLR signaling [31], including many of the same genes for cytokines and signal transduction molecules found to be expressed in response to NLP treatment in our study. Thus, there is precedent for robust changes in the expression of immunostimulatory genes following nanoparticle administration. What remains to be elucidated is how the NLP-induced changes in gene expression relate to downstream immune responses (i.e. production of cytokines and surface expression of activation markers on APCs). Whereas large changes in gene expression were detected in the spleen following IP administration of NLPs, proinflammatory cytokine levels in the serum were minimal (Fig. 4A) and no increase was observed in the surface expression of activation markers on splenic APCs (Fig. 4B). Moreover, the changes in gene expression induced by CpG:NLPs and MPLA:NLPs were comparable to NLPs alone, yet high levels of serum cytokines and robust upregulation of activation markers were observed following administration of both agonist:NLP complexes. Further work is required to understand the impact of these NLP-dependent transcriptional changes, and whether these responses are short lived, or translate into as of now unknown cellular outputs that have significant physiological consequences at the cellular and organismal level when TLR agonists are present in the NLPs.

Our data clearly demonstrate that conjugation to NLPs enhances innate immune responses to TLR agonists and further investigation will be necessary to elucidate the mechanism/s responsible for this enhancement. One possible method of enhancement could be related to the clustering together of multiple molecules of MPLA or CpG. When a cell encounters one NLP it is effectively encountering 3 molecules of MPLA or 9 molecules of CpG (Fig. 1C and F). This increase in local concentration of agonists may result in higher levels of activation on a per cell basis. Furthermore, our data demonstrate that NLPs enhance uptake of CpG into macrophages and dendritic cells (Fig. 6E and F), which may result in increased activation levels as the receptor for CpG (TLR9) is intracellular. RT-PCR analysis of immunoregulatory genes suggests that the NLP particles themselves may be an innate immune agonist, and therefore the enhancement could in part be due to a synergistic effect of simultaneous delivery of multiple agonists. The *in vivo* response to agonist:NLP constructs may be further augmented by enhanced trafficking of agonists to secondary lymphoid organs. Our data demonstrating higher percentages of splenocytes positive for CpG-Quasar 670 upon injection with CpG-Quasar 670:NLP versus CpG-Quasar 670 alone is likely due, in part, to the enhancement in uptake promoted by NLP conjugation. However, we cannot rule out the possibility that NLP conjugation also enhances trafficking of CpG to the spleen. Furthermore, conjugation to NLPs may result in retention of CpG in the spleen for longer periods of time. This is an interesting hypothesis given that the most significant differences in percent CpG-670^+ total splenocytes, macrophages and dendritic cells were seen at 24 and 48 h post injection (Fig. 6A–D). Likewise, further investigation is also needed to understand the mechanisms by which CpG:NLP complexes protect against lethal influenza challenge. Prophylactic initiation of innate immunity as a means of preventing or ameliorating disease caused by viral infection can be postulated to be effective by several means, including the induction of type I interferon-dependent antiviral mechanisms, activation of NK cells and stimulation of Th1 type-antiviral T cell responses [52]. The CpG used in these experiments was of the B class, therefore not likely to elicit large amounts of IFN-α [53]. Thus, investigation into the effects on anti-viral T cell and NK cell responses in the lungs will be key to understanding the mechanisms behind CpG:NLP mediated protection against influenza infection.

The goal of this study was to demonstrate that NLP conjugation enhances the efficacy of innate immune activation by TLR agonists and further demonstrate the utility of the NLP platform for immune modulation strategies. While transient activation of innate immune responses *in vivo* may be useful in certain scenarios and for specific populations [3], we recognize that this approach could also potentially drive adverse reactions in healthy human populations. While our data demonstrate the potential utility of NLP-based innate immune modulation, inbred mice do not represent the heterogeneity present in the human population. Specifically, mouse models cannot capture the complexity present in humans with respect to genetic background, previous exposures to infectious agents as well as the composition of an individual's microbiota [54]. All of these factors would likely result in a heterogeneous lymphocyte population where TLR stimulation could have pleiotropic effects that would be largely unpredictable. Therefore, translation to a clinical setting would require further refinement and a systematic optimization of the agonist:NLP to minimize the potential for any deleterious side effects.

5. Conclusions

In this study, we investigated the impact of TLR agonist:NLP complexes on innate immune responses *in vitro* and *in vivo*. We demonstrated that CpG and MPLA can be readily incorporated and accurately quantified within the NLP platform. Administration of CpG:NLP and MPLA:NLP versus the administration of free CpG and MPLA resulted in significant enhancement of multiple hallmarks of innate immune activation, including cytokine production, surface expression of activation markers, and transcriptional changes of immunoregulatory genes. Importantly, NLP conjugation enhanced cytokine production in response to both agonists not only in mice, but also in primary human dendritic cells. Finally, utilizing a mouse model of influenza, we demonstrate that prophylactic administration of CpG:NLP complexes provided complete protection from an otherwise lethal infection. The efficacy of CpG:NLP complexes at ameliorating infection, coupled with the observation that CpG:NLP and MPLA:NLP enhance innate immune responses not only in the murine system but also within primary human dendritic cells, indicate potential for the future clinical applications of the NLP platform as an innate immune modulator.

Acknowledgments

This work was performed under the auspices of the U.S. Department of Energy by Lawrence Livermore National Laboratory under contract DE-AC52-07NA27344 and supported by Laboratory Directed Research and Development grants 11-ERD-016 to A.R. and 11-LW-015 to N.O.F. from Lawrence Livermore National Laboratory and grant HHSN266200700008 to A.J.S. from the National Institutes of Health. LLNL-JRNL-642038.

Appendix A. Supplementary data

Supplementary data related to this article can be found at http://dx.doi.org/10.1016/j.biomaterials.2013.09.038.

References

[1] Thavaselvam D, Vijayaraghavan R. Biological warfare agents. J Pharm Bioallied Sci 2010;2:179–88.
[2] Lu S, Wang S. Technical transformation of biodefense vaccines. Vaccine 2009;27(Suppl. 4):D8–15.
[3] Hackett CJ. Innate immune activation as a broad-spectrum biodefense strategy: prospects and research challenges. J Allergy Clin Immunol 2003;112:686–94.
[4] Amlie-Lefond C, Paz DA, Connelly MP, Huffnagle GB, Dunn KS, Whelan NT, et al. Innate immunity for biodefense: a strategy whose time has come. J Allergy Clin Immunol 2005;116:1334–42.
[5] Treating infectious diseases in a microbial world: report of two workshops on novel antimicrobial therapeutics. The National Academies Press; 2006.
[6] Beutler B. Innate immunity: an overview. Mol Immunol 2004;40:845–59.
[7] Athman R, Philpott D. Innate immunity via toll-like receptors and nod proteins. Curr Opin Microbiol 2004;7:25–32.
[8] Olive C. Pattern recognition receptors: sentinels in innate immunity and targets of new vaccine adjuvants. Expert Rev Vaccines 2012;11:237–56.
[9] Parker LC, Prince LR, Sabroe I. Translational mini-review series on toll-like receptors: networks regulated by toll-like receptors mediate innate and adaptive immunity. Clin Exp Immunol 2007;147:199–207.
[10] Kanzler H, Barrat FJ, Hessel EM, Coffman RL. Therapeutic targeting of innate immunity with toll-like receptor agonists and antagonists. Nat Med 2007;13:552–9.
[11] Look M, Bandyopadhyay A, Blum JS, Fahmy TM. Application of nanotechnologies for improved immune response against infectious diseases in the developing world. Adv Drug Del Rev 2010;62:378–93.
[12] Dunne A, Marshall NA, Mills KHG. Tlr based therapeutics. Curr Opin Pharmocol 2011;11:404–11.
[13] Lembo A, Pelletier M, Iyer R, Timko M, Dudda JC, West TE, et al. Administration of a synthetic TLR4 agonist protects mice from pneumonic tularemia. J Immunol 2008;180:7574–81.
[14] Cole LE, Mann BJ, Shirey KA, Richard K, Yang Y, Gearhart PJ, et al. Role of TLR signaling in *francisella tularensis*-LPS-induced, antibody-mediated protection against *francisella tularensis* challenge. J Leukocyte Biol 2011;90:787–97.
[15] Airhart CL, Rohde HN, Bohach GA, Hovde CJ, Deobald CF, Lee SS, et al. Induction of innate immunity by lipid a mimetics increases survival from pneumonic plague. Microbiology 2008;154:2131–8.
[16] Jiang T, Zhao H, Li X-F, Deng Y-Q, Liu J, Xu L-J, et al. CpG oligodeoxynucleotides protect against the 2009 H1N1 pandemic influenza virus infection in a murine model. Antiviral Res 2011;89:124–6.
[17] Judy BM, Taylor K, Deeraksa A, Johnston RK, Endsley JJ, Vijayakumar S, et al. Prophylactic application of cpg oligonucleotides augments the early host response and confers protection in acute melioidosis. PLoS ONE 2012;7:e34176.
[18] Juffermans NP, Leemans JC, Florquin S, Verbon A, Kolk AH, Speelman P, et al. Cpg oligodeoxynucleotides enhance host defense during murine tuberculosis. Infect Immun 2002;70:147–52.
[19] Krieg AM, Love-Homan L, Yi A-K, Harty JT. Cpg DNA induces sustained IL-12 expression in vivo and resistance to listeria monocytogenes challenge. J Immunol 1998;161:2428–34.
[20] McCluskie MJ, Cartier JLM, Patrick AJ, Sajic D, Weeratna RD, Rosenthal KL, et al. Treatment of intravaginal hsv-2 infection in mice: a comparison of CpG oligodeoxynucleotides and resiquimod (r-848). Antiviral Res 2006;69:77–85.
[21] Wong JP, Christopher ME, Viswanathan S, Karpoff N, Dai X, Das D, et al. Activation of toll-like receptor signaling pathway for protection against influenza virus infection. Vaccine 2009;27:3481–3.
[22] Zimmermann S, Egeter O, Hausmann S, Lipford GB, Röcken M, Wagner H, et al. Cutting edge: CpG oligodeoxynucleotides trigger protective and curative Th1 responses in lethal murine leishmaniasis. J Immunol 1998;160:3627–30.
[23] Norton EB, Clements JD, Voss TG, Cárdenas-Freytag L. Prophylactic administration of bacterially derived immunomodulators improves the outcome of influenza virus infection in a murine model. J Virol 2010;84:2983–95.
[24] Klinman DM, Conover J, Coban C. Repeated administration of synthetic oligodeoxynucleotides expressing CpG motifs provides long-term protection against bacterial infection. Infect Immun 1999;67:5658–63.
[25] Elkins KL, Rhinehart-Jones TR, Stibitz S, Conover JS, Klinman DM. Bacterial DNA containing CpG motifs stimulates lymphocyte-dependent protection of mice against lethal infection with intracellular bacteria. J Immunol 1999;162:2291–8.
[26] Bode C, Zhao G, Steinhagen F, Kinjo T, Klinman DM. CpG DNA as a vaccine adjuvant. Expert Rev Vaccines 2011;10:499–511.
[27] Krishnamachari Y, Geary S, Lemke C, Salem A. Nanoparticle delivery systems in cancer vaccines. Pharm Res 2011;28:215–36.
[28] Jong S, Chikh G, Sekirov L, Raney S, Semple S, Klimuk S, et al. Encapsulation in liposomal nanoparticles enhances the immunostimulatory, adjuvant and antitumor activity of subcutaneously administered CpG ODN. Cancer Immunol Immunother 2007;56:1251–64.
[29] Harris J, Sharp FA, Lavelle EC. The role of inflammasomes in the immunostimulatory effects of particulate vaccine adjuvants. Eur J Immunol 2010;40:634–8.
[30] Lin AY, Mattos Almeida JP, Bear A, Liu N, Luo L, Foster AE, et al. Gold nanoparticle delivery of modified CpG stimulates macrophages and inhibits tumor growth for enhanced immunotherapy. PLoS ONE 2013;8:e63550.
[31] Hamasaki T, Uto T, Akagi T, Akashi M, Baba M. Modulation of gene expression related to toll-like receptor signaling in dendritic cells by poly(γ-glutamic acid) nanoparticles. Clin Vaccine Immunol 2010;17:748–56.
[32] Lung exposure of titanium dioxide nanoparticles induces innate immune activation and long-lasting lymphocyte response in the dark agouti rat. J Immunotoxicol 2011;8:111–21.
[33] Santos DM, Carneiro MW, de Moura TR, Soto M, Luz NF, Prates DB, et al. Plga nanoparticles loaded with kmp-11 stimulate innate immunity and induce the killing of leishmania. Nanomed Nanotechnol Biol Med 2013.

[34] Shima F, Uto T, Akagi T, Akashi M. Synergistic stimulation of antigen presenting cells via TLR by combining cpg odn and poly(γ-glutamic acid)-based nanoparticles as vaccine adjuvants. Bioconjug Chem 2013;24:926–33.
[35] Li H, Willingham SB, Ting JP-Y, Re F. Cutting edge: inflammasome activation by alum and alum's adjuvant effect are mediated by nlrp3. J Immunol 2008;181:17–21.
[36] Sharp FA, Ruane D, Claass B, Creagh E, Harris J, Malyala P, et al. Uptake of particulate vaccine adjuvants by dendritic cells activates the nalp3 inflammasome. Proc Natl Acad Sci U S A 2009;106:870–5.
[37] Eisenbarth SC, Colegio OR, O'Connor W, Sutterwala FS, Flavell RA. Crucial role for the nalp3 inflammasome in the immunostimulatory properties of aluminium adjuvants. Nature 2008;453:1122–6.
[38] Blanchette C, Segelke B, Fischer N, Corzett M, Kuhn E, Cappuccio J, et al. Characterization and purification of polydisperse reconstituted lipoproteins and nanolipoprotein particles. Int J Mol Sci 2009;10:2958–71.
[39] Blanchette CD, Law R, Benner WH, Pesavento JB, Cappuccio JA, Walsworth V, et al. Quantifying size distributions of nanolipoprotein particles with single-particle analysis and molecular dynamic simulations. J Lipid Res 2008;49:1420–30.
[40] Fischer NO, Rasley A, Corzett M, Hwang MH, Hoeprich PD, Blanchette CD. Colocalized delivery of adjuvant and antigen using nanolipoprotein particles enhances the immune response to recombinant antigens. J Am Chem Soc 2013;135:2044–7.
[41] Ryan RO. Nanodisks: hydrophobic drug delivery vehicles. Expert Opin Drug Deliv 2008;5:343–51.
[42] Cormode DP, Chandrasekar R, Delshad A, Briley-Saebo KC, Calcagno C, Barazza A, et al. Comparison of synthetic high density lipoprotein (HDL) contrast agents for mr imaging of atherosclerosis. Bioconjug Chem 2009;20:937–43.
[43] Bhattacharya P, Grimme S, Ganesh B, Gopisetty A, Sheng JR, Martinez O, et al. Nanodisc-incorporated hemagglutinin provides protective immunity against influenza virus infection. J Virol 2010;84:361–71.
[44] Fischer NO, Blanchette CD, Chromy BA, Kuhn EA, Segelke BW, Corzett M, et al. Immobilization of his-tagged proteins on nickel-chelating nanolipoprotein particles. Bioconjug Chem 2009;20:460–5.
[45] Blanchette CD, Fischer NO, Corzett M, Bench G, Hoeprich PD. Kinetic analysis of his-tagged protein binding to nickel-chelating nanolipoprotein particles. Bioconjug Chem 2010;21:1321–30.
[46] Vorauer-Uhl K, Jeschek D, Lhota G, Wagner A, Strobach S, Katinger H. Simultaneous quantification of complex phospholipid compositions containing monophosphoryl lipid-A by RP-HPLC. J Liq Chromatogr Rel Technol 2009;32:2203–15.
[47] Ray A, Dittel BN. Isolation of mouse peritoneal cavity cells. J Vis Exp 2010: e1488.
[48] Lu H, Dietsch GN, Matthews M-AH, Yang Y, Ghanekar S, Inokuma M, et al. Vtx-2337 is a novel TLR8 agonist that activates NK cells and augments ADCC. Clin Cancer Res 2012;18:499–509.
[49] Chan JF-W, Lau SK-P, Woo PC-Y. The emerging novel middle east respiratory syndrome coronavirus: The "knowns" and "unknowns". J Formosan Med Assoc.
[50] Leleux J, Roy K. Micro and nanoparticle-based delivery systems for vaccine immunotherapy: an immunological and materials perspective. Adv Healthc Mater 2013;2:72–94.
[51] Demento SL, Eisenbarth SC, Foellmer HG, Platt C, Caplan MJ, Mark Saltzman W, et al. Inflammasome-activating nanoparticles as modular systems for optimizing vaccine efficacy. Vaccine 2009;27:3013–21.
[52] Stetson DB, Medzhitov R. Type I interferons in host defense. Immunity 2006;25:373–81.
[53] Krieg AM. CpG motifs in bacterial DNA and their immune effects. Annu Rev Immunol 2002;20:709–60.
[54] Mestas J, Hughes CCW. Of mice and not men: differences between mouse and human immunology. J Immunol 2004;172:2731–8.